A Memristive System with Hidden Attractors and Its Engineering Application

Viet-Thanh Pham, Sundarapandian Vaidyanathan, Christos Volos, Esteban Tlelo-Cuautle and Fadhil Rahma Tahir

Abstract After the successful fabrication of memristor at Hewlett–Packard Laboratories, memristor—based systems and their potential applications have been getting a great deal of attention in different areas from associative memory, neural networks, programmable analog ICs to low–power computing and so on. It is well known that the presence of memristor in a dynamical system may yield novel features because it is both a nonlinear element and a memory element. In this chapter, we present a memristive system with an infinite number of equilibrium points. From the computing view of point, such system belongs to a class of systems with hidden attractors according to a new classification of nonlinear dynamics. This classification has proposed by Leonov and Kuznetsov and played a significant role in engineering applications. In this work, we study the complex dynamics of the introduced memristive system. It is worth noting that the proposed system can generate hyperchaotic behavior which will be used for image encryption to illustrate its engineering application. The chaos–based image encryption has many applications in digital image storing, medical image databases, video conferencing or military transmit systems.

V.-T. Pham (✉)
School of Electronics and Telecommunications, Hanoi University of Science and Technology, Hanoi, Vietnam
e-mail: pvt3010@gmail.com

S. Vaidyanathan
Research and Development Centre, Vel Tech University, Chennai, Tamil Nadu, India
e-mail: sundarcontrol@gmail.com

C. Volos
Physics Department, Aristotle University of Thessaloniki, Thessaloniki, Greece
e-mail: volos@physics.auth.gr

E. Tlelo-Cuautle
Department of Electronics, INAOE, Tonantzintla Puebla 72840, Mexico
e-mail: etlelo@inaoep.mx

F.R. Tahir
Department of Electrical Engineering, College of Engineering University of Basrah, Basrah, Iraq
e-mail: fadhilrahma.creative@gmail.com

S. Vaidyanathan and C. Volos (eds.), *Advances in Memristors, Memristive Devices and Systems*, Studies in Computational Intelligence 701,
DOI 10.1007/978-3-319-51724-7_4

Keywords Chaos · Hyperchaos · Lyapunov exponents · Bifurcation · Hidden attractor · Equilibrium · Memristor · Encryption · Security

1 Introduction

In the past few decades, various chaotic systems have been investigated, for example: Lorenz system (Lorenz 1963), Rössler system (Rössler 1976), Arneodo system (Arneodo et al. 1981), Chen system (Chen and Ueta 1999), Lü system (Lü and Chen 2002), Vaidyanathan system (Vaidyanathan 2013), time–delay systems (Barnerjee et al. 2012), Tacha system (Tacha et al. 2016), jerk systems (Vaidyanathan et al. 2014). In addition, hyperchaotic systems have been discovered (Rössler 1979). Hyperchaotic system is characterized by more than one positive Lyapunov exponent. Therefore hyperchaotic system can exhibit a higher level of complexity with respect to chaotic system (Vaidyanathan and Azar 2015). Hyperchaos is better than conventional chaos in a variety of areas, for example, hyperchaos increases the security of chaotic–based communication systems significantly (Udaltsov et al. 2003; Sadoudi et al. 2013) or encryption algorithm based on hyperchaos is safer than one based on chaos (Gao and Chen 2008). Moreover hyperchaos has been applied in different areas such as cryptosystems (Grassi and Mascolo 1999), neural networks (Huang and Yang 2006), secure communications (Udaltsov et al. 2003; Sadoudi et al. 2013), or laser design (Vicente et al. 2005).

The realization of memristor at Hewlett–Packard Labs promotes potential memristor—based applications (Strukov et al. 2008). Some attractive memristor—based applications are high–speed low–power processors (Yang et al. 2013), adaptive filter (Driscoll et al. 2010), pattern recognition systems (Corinto et al 2012), associative memory (Pershin and Ventra 2010), neural networks (Adhikari et al. 2012; Ascoli and Corinto 2013), and programmable analog integrated circuits (Shin et al. 2011). Especially, the intrinsic nonlinear characteristic of memristor has been exploited in designing hyperchaotic oscillators (Buscarino et al. 2012a; Fitch et al. 2012). Hyperchaos was generated by combining a memristor with cubic nonlinear characteristics and a modified canonical Chua's circuit (Fitch et al. 2012). This memristor—based modified canonical Chua's circuit is a five–dimensional hyperchaotic oscillator. By extending the HP memristor—based canonical Chua's oscillator, a six–dimensional hyperchaotic oscillator was designed (Buscarino et al. 2012b). Authors used a configuration based on two HP memristors in antiparallel (Buscarino et al. 2012a). Four–dimensional hyperchaotic memristive systems were discovered by Li et al. (2014, 2015). A 4D memristive system with a line of equilibrium points was presented in Li et al. (2014) while another memristive system with an uncountable infinite number of stable and unstable equilibria was reported in Li et al. (2015). Interestingly, memristor—based hyperchaotic systems without equilibrium were introduced in Pham et al. (2014b; 2015). These memristive systems belong to a new category of chaotic systems with hidden attractors (Leonov et al. 2011; Leonov and Kuznetsov 2013). Hidden attractor cannot be found by using a

numerical method in which a trajectory started from a point on the unstable manifold in the neighbourhood of an unstable equilibrium (Jafari and Sprott 2013). Thus hidden attractors play an important role in many fields such as in mechanics, secure communication and electronics (Kuznetsov et al. 2011; Leonov et al. 2011; Pham et al. 2014a, c; Sharma et al. 2015).

In this chapter, we study a system based on a memristive device and its application. It is interesting that the memristive system has an infinite number of equilibrium points and can generate hyperchaos. This chapter is organized as follows. Section 2 presents the description of the memristive system. Dynamics and properties of such memristive system are investigated in Sect. 3. We implement an image encryption scheme based on the memeristive system in Sect. 4 and discuss its security in Sect. 5. Finally, conclusions are drawn in Sect. 6.

2 Description of the Proposed System

According to studies of (Chua 1971; Chua and Kang 1976), a memristive system is defined by

$$\begin{cases} \dot{w} = f(w, y, t) \\ h(w, y) = g(w, y, t)\, y, \end{cases} \tag{1}$$

where y, $h(w, y)$, w are the input, output, and internal state of the memristive device. The functions f and g are a continuous n–dimensional vector function and a continuous scalar function.

Based on the definition of memristive system, recently authors have introduced a novel memrisitve system (Pham et al. 2014b) in the following form:

$$\begin{cases} \dot{x} = -10x - ay - yz \\ \dot{y} = -6x + 1.2xz + 0.1h(w, y) + b \\ \dot{z} = -z - 1.2xy \\ \dot{w} = y, \end{cases} \tag{2}$$

where a and b are two positive real parameters. Here $h(w, y)$ is the output of the memristive device described by

$$\begin{cases} \dot{w} = y \\ h(w, y) = \left(1 + 0.24w^2 - 0.0016w^4\right) y. \end{cases} \tag{3}$$

As have been known system (2) can display hyperchaotic attractors without equilibrium for $b \neq 0$ (Pham et al. 2014b). In addition, dynamics of the memristive system without equilibrium have been investigated by using numerical simulations and circuital implementation (Pham et al. 2014b).

When $b = 0$, the system (2) can be rewritten by

$$\begin{cases} \dot{x} = -10x - ay - yz \\ \dot{y} = -6x + 1.2xz + 0.1\left(1 + 0.24w^2 - 0.0016w^4\right)y \\ \dot{z} = -z - 1.2xy \\ \dot{w} = y. \end{cases} \tag{4}$$

It is easy to get the equilibrium points of system (4) by solving $\dot{x} = 0$, $\dot{y} = 0$, $\dot{z} = 0$, and $\dot{w} = 0$, that is

$$-10x - ay - yz = 0, \tag{5}$$

$$-6x + 1.2xz + 0.1\left(1 + 0.24w^2 - 0.0016w^4\right)y = 0, \tag{6}$$

$$-z - 1.2xy = 0, \tag{7}$$

$$y = 0, \tag{8}$$

From Eq. (8), we have $y = 0$. By substituting $y = 0$ in Eq. (5), it leads to $x = 0$. As result, we get $z = 0$ from Eq. (7). In addition, Eq. (6) insists and does not depend on w. In other words, system (4) has an infinite number of equilibrium points

$$E\left(0, 0, 0, w\right). \tag{9}$$

Moreover, the equilibrium points are located on a line.

System (4) belongs to a new class of systems with hidden attractor from a computational point of view (Jafari and Sprott 2013). The basin of the system may intersect the line equilibrium in some sections. But there are uncountable points on the line that are outside the basin of attraction. Thus the knowledge about equilibrium points does not help in their localization (Jafari and Sprott 2013).

In the next section, we present complex dynamics of the memristive system with infinite equilibria (4).

3 Dynamics of the Memristive System

When choosing the parameter $a = 5$ and the initial condition

$$\left(x\left(0\right), y\left(0\right), z\left(0\right), w\left(0\right)\right) = \left(0, 0.01, 0.01, 0\right), \tag{10}$$

the calculated Lyapunov exponents of system (4) are

$$L_1 = 0.1364,\ L_2 = 0.0071,\ L_3 = 0,\ L_4 = -10.8584. \tag{11}$$

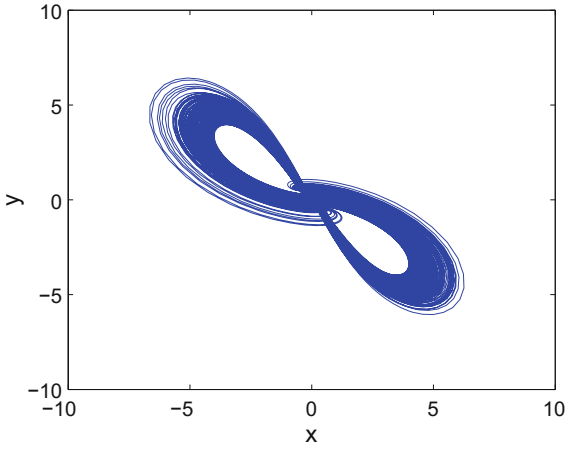

Fig. 1 2–D projection of the hyperchaotic memristive system with an infinite number of equilibrium points (4) in the (x, y)–plane

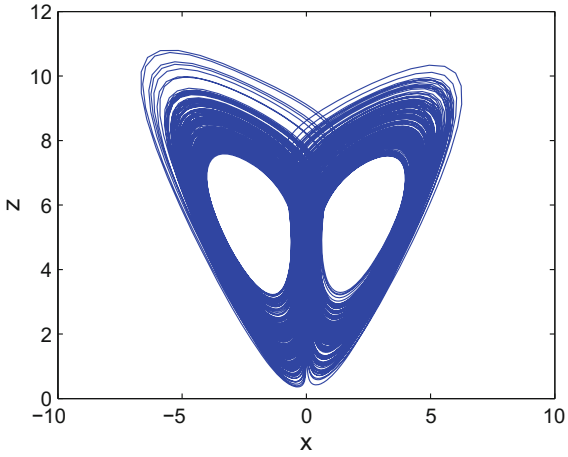

Fig. 2 2–D projection of the hyperchaotic memristive system with an infinite number of equilibrium points (4) in the (x, z)–plane

Therefore, system (4) is a four–dimensional hyperchaotic system because there are two positive Lyapunov exponents, one zero and one negative Lyapunov exponent. Figures 1, 2, 3 and 4 display 2–D projections of the hyperchaotic attractors with an infinite number of equilibrium points.

It has been known that the Kaplan–Yorke fractional dimension presenting the complexity of attractor is given by

$$D_{KY} = j + \frac{1}{\left|L_{j+1}\right|} \sum_{i=1}^{j} L_i, \tag{12}$$

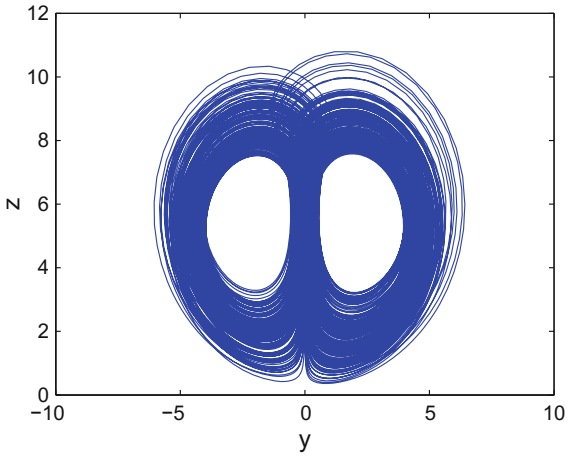

Fig. 3 2–D projection of the hyperchaotic memristive system with an infinite number of equilibrium points (4) in the (y, z)–plane

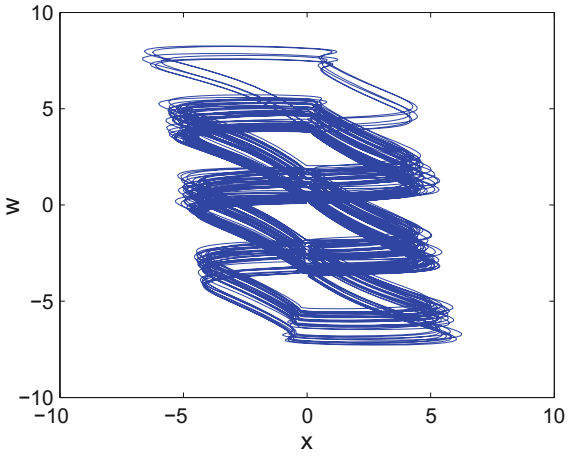

Fig. 4 2–D projection of the hyperchaotic memristive system with an infinite number of equilibrium points (4) in the (x, w)–plane

where j is the largest integer satisfying $\sum_{i=1}^{j} L_i \geq 0$ and $\sum_{i=1}^{j+1} L_i < 0$. The calculated Kaplan–Yorke fractional dimension of system (4) for $a = 5$ is

$$D_{KY} = 3 + \frac{L_1 + L_2 + L_3}{|L_4|} = 3.0132, \tag{13}$$

which indicated a strange attractor. Poincaré maps of system (4) are also illustrated in Figs. 5, 6 and 7. As can be seen from the Poincaré maps, the memristive system (4) has complex dynamics.

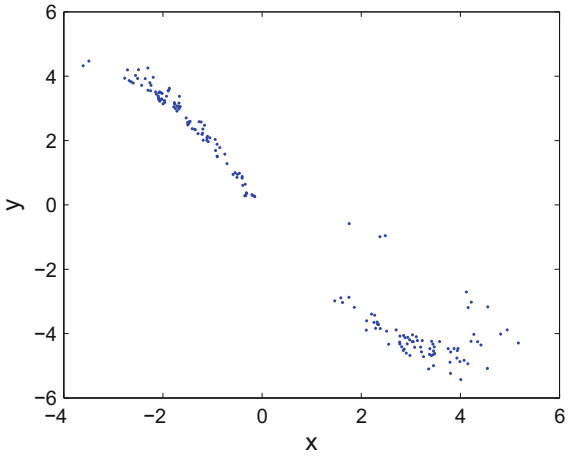

Fig. 5 Poincaré map of the hyperchaotic memristive system with an infinite number of equilibrium points (4) in the (x, y)–plane

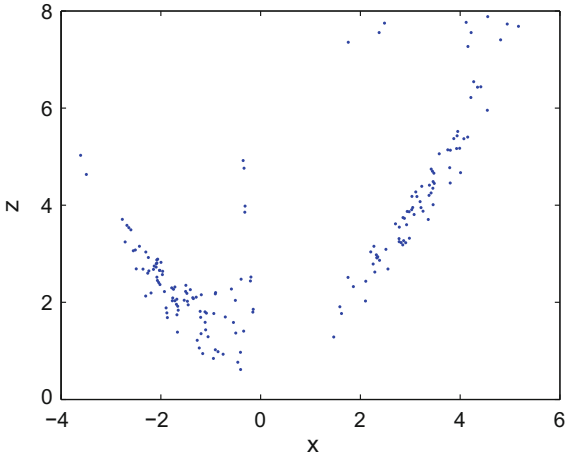

Fig. 6 Poincaré map of the hyperchaotic memristive system with an infinite number of equilibrium points (4) in the (x, z)–plane

We discover detail dynamics of system (4) by using bifurcation diagram and Lyapunov exponents. The bifurcation diagram of the variable z and the corresponding Lyapunov exponents are reported in Figs. 8, 9 and 10. The system (4) performs periodic state, chaos, and hyperchaos when varying the parameter a from 1 to 6. The system displays limit cycle for $a \in [1, 1.46]$, $[1.5, 1.96]$, $[2.48, 2.88]$. For example, periodical states of system (4) for $a = 2.6$ are presented in Figs. 11, 12, 13 and 14. Chaotic behavior can be observed for $a \in [3.06, 3.34]$, $(4.66, 4.78)$. The system can exhibits hyperchaotic behavior for $a \in [4.08, 4.66]$, $[4.78, 6]$.

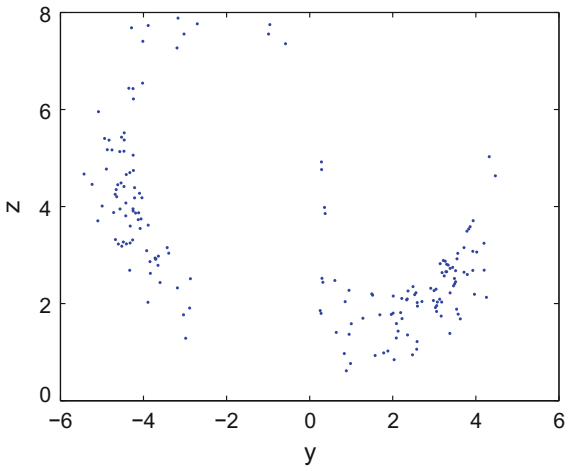

Fig. 7 Poincaré map of the hyperchaotic memristive system with an infinite number of equilibrium points (4) in the (y, z)–plane

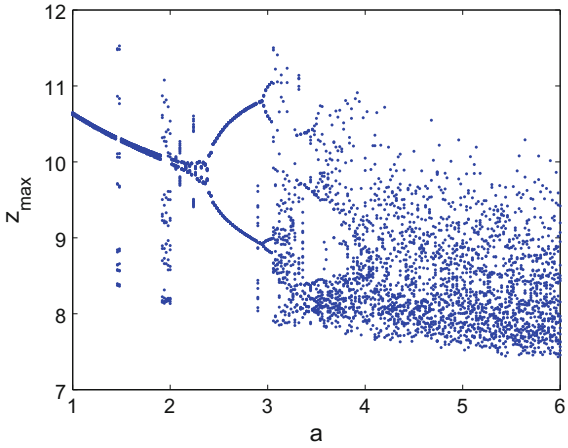

Fig. 8 Bifurcation diagram of the hyperchaotic memristive system with an infinite number of equilibrium points (4) when changing the parameter a

4 Application of the Proposed System

Nowadays, digital image information has become popular in the world because of the rapid development of Internet. In many applications such as military images, online personal photographs, or fingerprint images of authentication systems, it has to meet the requirements of safety and security (Volos et al. 2013). Therefore, numerous encryption techniques, especially chaos–based encryption, have been proposed and implemented (Liao et al. 2010; Matthews 1989; Seyedzadeh et al. 2012; Tong and Cui 2009; Wang et al. 2012; Yeung and Pankanti 2000; Zhang et al. 2005).

In this section, we use the encryption scheme suggested by Gao and Chen (Gao and Chen 2008) to illustrate a possible application of the proposed memristive sys-

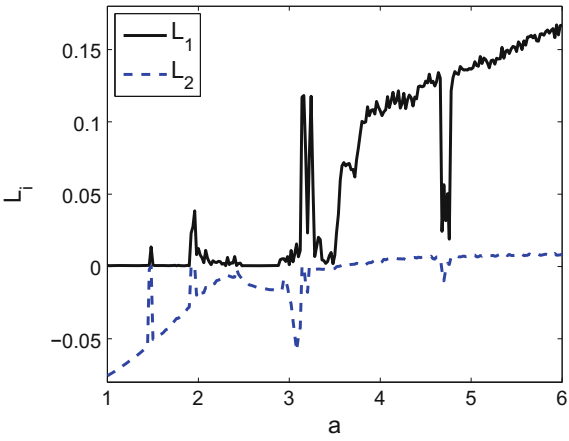

Fig. 9 Two largest Lyanpunov exponents of the hyperchaotic memristive system with an infinite number of equilibrium points (4) when varying the parameter a

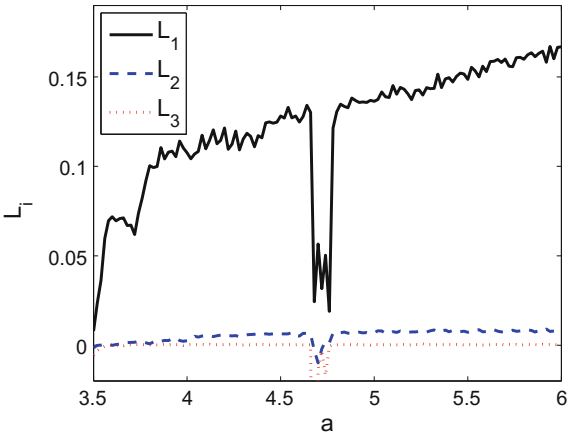

Fig. 10 Three largest Lyanpunov exponents of the hyperchaotic memristive system with an infinite number of equilibrium points (4) when varying the parameter a

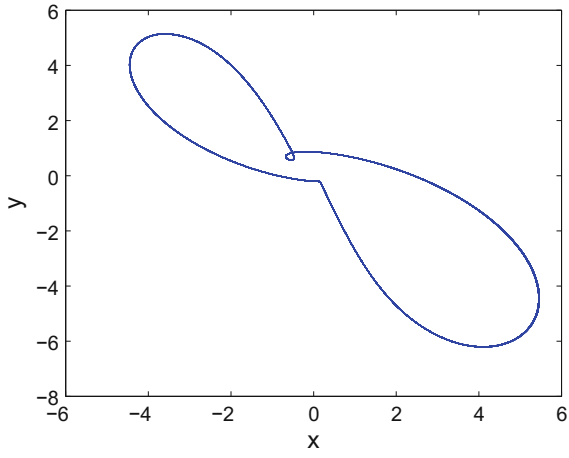

Fig. 11 Limit cycle of the hyperchaotic memristive system with an infinite number of equilibrium points (4) in the (x, y)–plane for $a = 2.6$

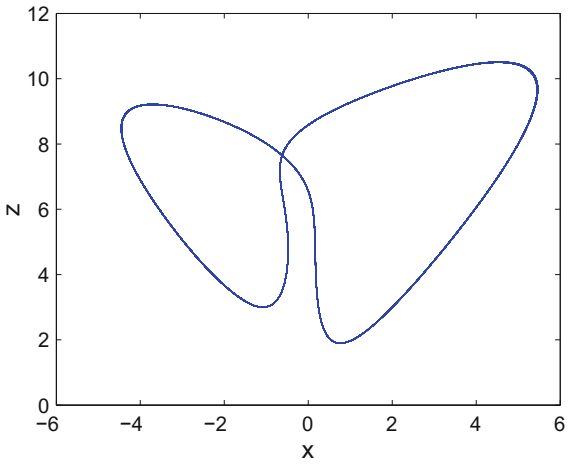

Fig. 12 Limit cycle of the hyperchaotic memristive system with an infinite number of equilibrium points (4) in the (x, z)–plane for $a = 2.6$

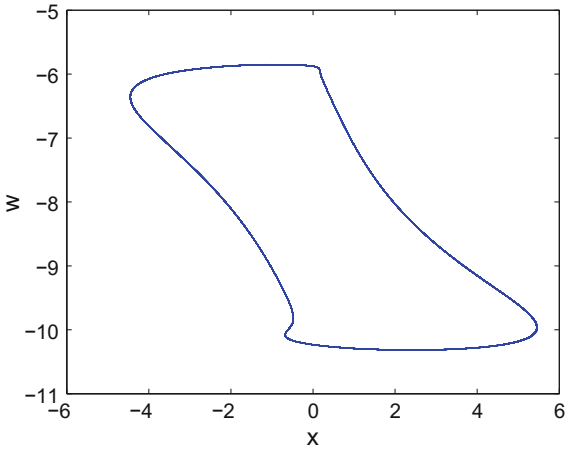

Fig. 13 Limit cycle of the hyperchaotic memristive system with an infinite number of equilibrium points (4) in the (x, w)–plane for $a = 2.6$

tem. We consider a plain–image with the dimension $N \times M$. The position matrix of pixels, which presents the grey value of the image is denoted as $P_{i,j}(I)$.

The encryption includes two steps as illustrated in Fig. 15.

Step 1: The main purpose of the step 1 is to shuffle the position of the plain image. This step is based on a chaotic map (Gao and Chen 2008).

Firstly, we do some iterations based on the Logistic map

$$x_{n+1} = 4x_n \left(1 - x_n\right), \tag{14}$$

to get a new value x_0. Then we calculate a value of h:

$$h = \text{mod}\left(x_0 \times 10^{14}, M\right), \tag{15}$$

in which the function mod(.) returns the remainder after division.

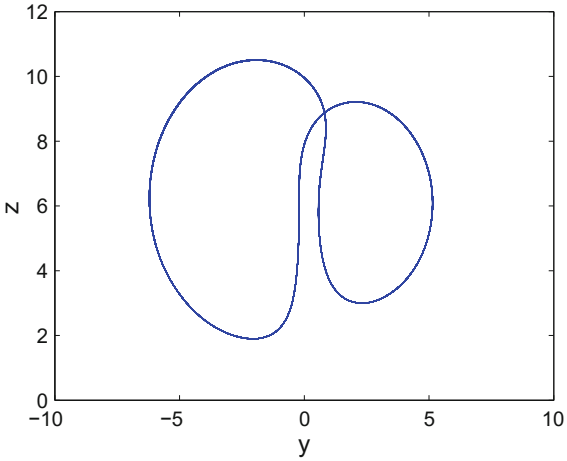

Fig. 14 Limit cycle of the hyperchaotic memristive system with an infinite number of equilibrium points (4) in the (y, z)–plane for $a = 2.6$

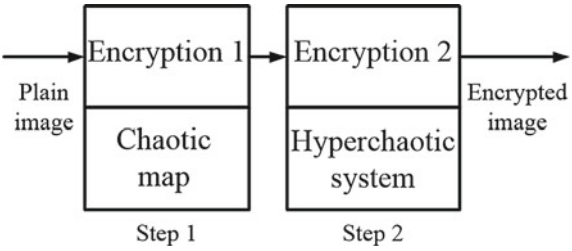

Fig. 15 Block diagram of the encryption scheme including two steps. The first step is based on a chaotic map while the second step is based on a hyperchaotic system

Secondly, we obtain M different data by repeating (15). These obtained data are reordered in $\{h_i,\ i = 1, 2, \ldots, M\}$ where $h_i \neq h_j$ if $i \neq j$. Then the rows of position matrix $P_{i,j}$ are rearranged by using $\{h_i,\ i = 1, 2, \ldots, M\}$. In other words, we create a new image position matrix $P^h_{i,j}$ based on row transformation. After that we shuffle the column position of the image for every row of the new position matrix $P^h_{i,j}$ with the same approach.

Thirdly, we do the iteration of Logistic map to calculate the value of l by using:

$$l = \mathrm{mod}\left(x_0 \times 10^{14}, N\right). \tag{16}$$

Fourthly, we repeat the iteration of Logistic map and (16) to get N different data. These data are reordered in $\{l_i,\ i = 1, 2, \ldots, N\}$ where $l_i \neq l_j$ if $i \neq j$. Next the data of every column of position matrix $P^h_{i,j}$ are rearranged by using $\{l_i,\ i = 1, 2, \ldots, N\}$. In other words, we create a new column transformation of the first row of image position matrix $P^{hl}_{i,j}$.

Finally, by completing the column transformation for all rows, an image total shuffling matrix $P^{hl}_{i,j}$ is derived.

Step 2: The main purpose of the step 2 is to encrypt the shuffled image. This step is based on a hyperchaotic system (Gao and Chen 2008).

Firstly, we iterate the hyperchaotic memristive system (4) for N_0 times by applying the Runge–Kutta algorithm to eliminate the effect of transient procedure.

Secondly, we iterate the hyperchaotic memristive system (4) to get four state variables x, y, z, and w at the N_0 time. Four corresponding decimal fractions x, y, z, w are generated as

$$x = \mathrm{mod}\left((\mathrm{abs}\,(x) - \mathrm{floor}\,(\mathrm{abs}\,(x))) \times 10^{14}, 256\right), \tag{17}$$

$$y = \mathrm{mod}\left((\mathrm{abs}\,(y) - \mathrm{floor}\,(\mathrm{abs}\,(y))) \times 10^{14}, 256\right), \tag{18}$$

$$z = \mathrm{mod}\left((\mathrm{abs}\,(z) - \mathrm{floor}\,(\mathrm{abs}\,(z))) \times 10^{14}, 256\right), \tag{19}$$

$$w = \mathrm{mod}\left((\mathrm{abs}\,(w) - \mathrm{floor}\,(\mathrm{abs}\,(w))) \times 10^{14}, 256\right), \tag{20}$$

where abs(.) is the absolute function while the function floor(.) calculates the nearest integer.

Thirdly, the new serial numbers X, Y, Z, W are given by

$$X = \mathrm{mod}\,(x, 4), \tag{21}$$

$$Y = \mathrm{mod}\,(y, 4), \tag{22}$$

$$Z = \mathrm{mod}\,(z, 4), \tag{23}$$

$$W = \mathrm{mod}\,(w, 4). \tag{24}$$

Depending on the values of these new serial numbers, there are corresponding groups of states (B_1, B_2, B_3) to perform encryption. For instance, the combination of states (B_1, B_2, B_3) are (x, y, z), (x, y, w), (x, z, w), and (y, z, w) for the serial numbers 0, 1, 2, and 3, respectively. Then we apply the XOR operation between three bytes of the image total shuffling matrix $P^{hl}_{i,j}$ and three bytes of the selected group of three states as follows

$$\begin{cases} C_{3\times(i-1)+1} = P_{3\times(i-1)+1} \oplus B_1 \\ C_{3\times(i-1)+2} = P_{3\times(i-1)+2} \oplus B_2 \\ C_{3\times(i-1)+3} = P_{3\times(i-1)+3} \oplus B_3, \end{cases} \tag{25}$$

Fig. 16 Presentation of the plain image

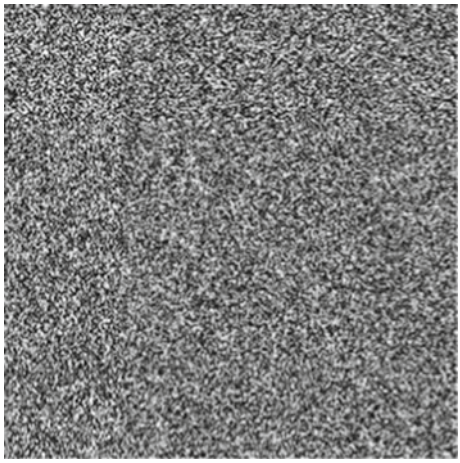

Fig. 17 Presentation of the encrypted image

in which P_j and $C_j, j = 1, 2, \ldots, N \times M$ indicate the pixels of the plain shuffled image and the ciphered image.

Finally, we continue doing the encryption until the whole image is encrypted.

We have applied the image encryption scheme to the plain–image with the size 256×256 (Fig. 16). We assume that the secret key is

$$\left(x(0), y(0), z(0), w(0), N_0\right) = (0, 0.01, 0.01, 0, 3000). \tag{26}$$

The encrypted image is obtained as illustrated in Fig. 17 while the decrypted image is shown in Fig. 18.

Fig. 18 Presentation of the decrypted image

5 Security Analysis

In this section, we consider the security of the image encryption scheme.

5.1 Key Space Analysis

Secret keys in the encryption scheme are the initial values of chaotic map and the hyperchaotic memristive system, as well as the systems' parameter values. In addition, secret keys can include the iteration number N_0. Thus, the key space is enough large to resist brute–force attacks.

5.2 Key Sensitivity

An intruder, who does not know the secret key, cannot recover the original plain image. In order to show the sensitivity of the encryption scheme to the secret key, we take an example where the intruder decrypts the encrypted image in Fig. 17 with the following secret key:

$$\left(x\left(0\right), y\left(0\right), z\left(0\right), w\left(0\right), N_0\right) = \left(0, 0.01, 0.01, 10^{-6}, 3000\right). \tag{27}$$

The failure of recovering the plain image by the intruder is illustrated in Fig. 19.

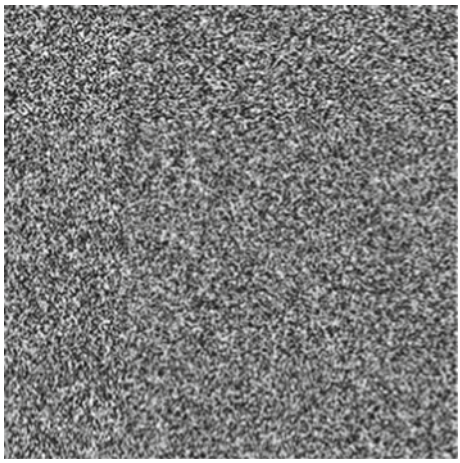

Fig. 19 The recovered image by an intruder

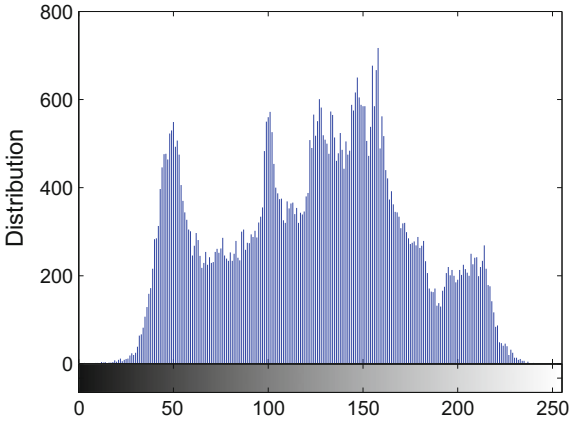

Fig. 20 Histogram of the plain image

5.3 Histogram Analysis

As have been known, two methods preventing the statistical attacks are the diffusion and confusion Shannon (1949). The histograms of the plain–image and the encrypted image are presented in Figs. 20, 21. It is easy to see that the histogram of the ciphered image is different from one of the plain–image. The histogram of the ciphered image has a uniform distribution which indicates the security of the encryption scheme from a statistical attack.

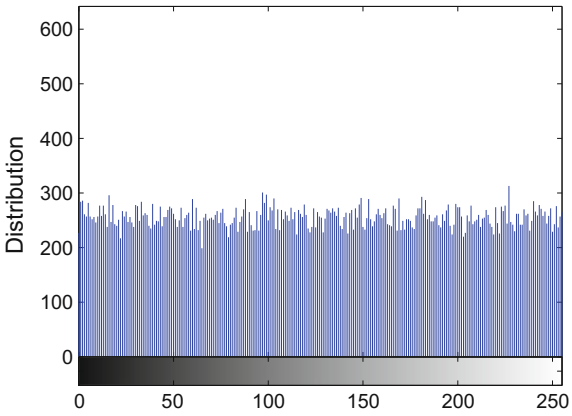

Fig. 21 Histogram of the encrypted image

5.4 Information Entropy

The entropy of a source is defined by

$$E(S) = -\sum_{i=0}^{N-1} p\left(s_i\right) \log_2 \left(p\left(s_i\right)\right), \tag{28}$$

with $p\left(s_i\right)$ is the possibility of appearance of the symbol s_i. Therefore, the information entropy of an image indicates the distribution of the gray scale values. The information entropy is much bigger when the distribution is much uniform. The calculated information entropy of the encrypted image is 7.9965. It is higher than the information entropy of the plain image (7.4888). The higher information entropy of the encrypted image presents the safety of the encryption scheme from an entropy attack (Volos et al. 2013).

6 Conclusion

In this chapter, a dynamical system with a memristive device has been studied. The system has many special features such as hyperchaos, a infinite number of equilibrium points, and hidden attractors due to the presence of the memristive device. Fundamental dynamical behaviors of the memristive system are discovered through calculating equilibrium points, phase portraits of hyperchaotic attractors, Poincaré maps, bifurcation diagram, Lyapunov exponents and Kaplan–Yorke dimension. The memristive system can be used in potential applications in secure communications and cryptography because of its complex behavior. In particular, we have implemented an image encryption scheme based on the hyperchaotic memristive system. In addition, security analysis of image encryption scheme are discussed. Further studies related to applications of this system will be presented in our future works.

Acknowledgements Viet–Thanh Pham would like to thank Le Thi Van Thu, Philips Electronics – Vietnam, for her help.

References

Adhikari, S. P., Yang, C., Kim, H., & Chua, L. O. (2012). Memristor bridge synapse-based neural network and its learning. *IEEE Transactions on Neural Networks and Learning Systems*, *23*, 1426–1435.

Arneodo, A., Coullet, P., & Tresser, C. (1981). Possible new strange attractors with spiral structure. *Communications in Mathematical Physics*, *79*, 573–579.

Ascoli, A., & Corinto, F. (2013). Memristor models in a chaotic neural circuit. *International Journal of Bifurcation and Chaos*, *23*, 1350052.

Barnerjee, T., Biswas, D., & Sarkar, B. C. (2012). Design and analysis of a first order time-delayed chaotic system. *Nonlinear Dynamics*, *70*, 721–734.

Buscarino, A., Fortuna, L., Frasca, M., & Gambuzza, L. V. (2012a). A chaotic circuit based on Hewlett–Packard memristor. *Chaos*, *22*, 023136.

Buscarino, A., Fortuna, L., Frasca, M., & Gambuzza, L. V. (2012b). A gallery of chaotic oscillators based on hp memristor. *International Journal of Bifurcation and Chaos*, *22*, 1330015–14.

Chen, G., & Ueta, T. (1999). Yet another chaotic attractor. *International Journal of Bifurcation and Chaos*, *9*, 1465–1466.

Chua, L. O. (1971). Memristor-The missing circuit element. *IEEE Transactions Circuit Theory*, *18*, 507–519.

Chua, L. O., & Kang, S. M. (1976). Memristive devices and system. *Proceedings of the IEEE*, *64*, 209–223.

Corinto, F., Ascoli, A., & Gilli, M. (2012). Analysis of current-voltage characteristics for memristive elements in pattern recognition systems. *International Journal of Circuit Theory and Applications*, *40*, 1277–1320.

Driscoll, T., Quinn, J., Klien, S., Kim, H. T., Kim, B. J., Pershin, Y. V., et al. (2010). Memristive adaptive filters. *Applied Physics Letters*, *97*, 093502.

Shannon, C. E. (1949). Communication theory of secrecy system. *Journal of Bell Systems Technology*, *28*, 656–715.

Fitch, A. L., Yu, D., Iu, H. H. C., & Sreeram, V. (2012). Hyperchaos in an memristor-based modified canonical Chua's circuit. *International Journal of Bifurcation and Chaos*, *22*, 1250133–8.

Gao, T., & Chen, Z. (2008). A new image encryption algorithm based on hyper-chaos. *Physics Letters A*, *372*, 394–400.

Grassi, G., & Mascolo, S. (1999). A system theory approach for designing cryptosystems based on hyperchaos. *IEEE Transactions on Circuits and Systems I Fundamental Theory and Applications*, *46*, 1135–1138.

Huang, Y., & Yang, X. (2006). Hyperchaos and bifurcation in a new class of four-dimensional hopfield neural networks. *Neurocomputing*, *69*, 1787–1795.

Jafari, S., & Sprott, J. C. (2013). Simple chaotic flows with a line equilibrium. *Chaos, Solitons and Fractals*, *57*, 79–84.

Kuznetsov, N. V., Leonov, G. A., & Seledzhi, S. M. (2011). Hidden oscillations in nonlinear control systems. *IFAC Proceedings*, *18*, 2506–2510.

Leonov, G. A., & Kuznetsov, N. V. (2013). Hidden attractors in dynamical systems: From hidden oscillation in Hilbert-Kolmogorov, Aizerman and Kalman problems to hidden chaotic attractor in chua circuits. *International Journal of Bifurcation and Chaos*, *23*, 1330002.

Leonov, G. A., Kuznetsov, N. V., Kuznetsova, O. A., Seldedzhi, S. M., & Vagaitsev, V. I. (2011). Hidden oscillations in dynamical systems. *Transactions on Systems Control*, *6*, 54–67.

Li, Q., Hu, S., Tang, S., & Zeng, G. (2014). Hyperchaos and horseshoe in a 4D memristive system with a line of equilibria and its implementation. *International Journal of Circuit Theory and Applications*, *42*, 1172–1188.

Li, Q., Zeng, H., & Li, J. (2015). Hyperchaos in a 4D memristive circuit with infinitely many stable equilibria. *Nonlinear Dynamics*, *79*, 2295–2308.

Liao, X., Lai, S., & Zhou, Q. (2010). A novel image encryption algorithm based on self-adaptive wave transmission. *Signal Processing*, *90*, 2714–2722.

Lorenz, E. N. (1963). Deterministic non-periodic flow. *Journal of the Atmospheric Sciences*, *20*, 130–141.

Lü, J., & Chen, G. (2002). A new chaotic attractor coined. *International Journal of Bifurcation and Chaos*, *12*, 659–661.

Matthews, R. (1989). One the derivation of a chaotic encryption algorithm. *Cryptologia*, *8*, 29–42.

Pershin, Y. V., & Ventra, M. D. (2010). Experimental demonstration of associative memory with memristive neural networks. *Neural Networks*, *23*, 881–886.

Pham, V.-T., Jafari, S., Volos, C., Wang, X., & Golpayegani, S. M. R. H. (2014a). Is that really hidden? The presence of complex fixed-points in chaotic flows with no equilibria. *International Journal of Bifurcation and Chaos*, *24*, 1450146.

Pham, V.-T., Volos, C., & Gambuzza, L. V. (2014b). A memristive hyperchaotic system withou equilibrium. *The Scientific World Journal*, *2014*, 368986–9.

Pham, V.-T., Volos, C. K., Jafari, S., Wei, Z., & Wang, X. (2014c). Constructing a novel no-equilibrium chaotic system. *International Journal of Bifurcation and Chaos*, *24*, 1450073.

Pham, V. T., Volos, C. K., Vaidyanathan, S., Le, T. P., & Vu, V. Y. (2015). A memristor-based hyperchaotic system with hidden attractors: Dyamics, sychronization and circuital emulating. *Journal of Engineering Science and Technology Review*, *8*, 205–214.

Rössler, O. E. (1976). An equation for continuous chaos. *Physics Letters A*, *57*, 397–398.

Rössler, O. E. (1979). An equation for hyperchaos. *Physics Letters A*, *71*, 155–157.

Sadoudi, S., Tanougast, C., Azzaz, M. S., & Dandache, A. (2013). Design and FPGA implementation of a wireless hyperchaotic communication system for secure realtime image transmission. *EURASIP Journal on Image and Video Processing*, *943*, 1–18.

Seyedzadeh, S. M., Mirzakuchaki, S., & Fast, A. (2012). Color image encryption algorithm based on coupled two-dimensional piecewise chaotic map. *Signal Processing*, *92*, 1201–1215.

Sharma, P. R., Shrimali, M. D., Prasad, A., Kuznetsov, N. V., & Leonov, G. A. (2015). Control of multistability in hidden attractors. *The European Physical Journal Special Topics*, *224*, 1485–1491.

Shin, S., Kim, K., & Kang, S. M. (2011). Memristor applications for programmable analog ICs. *IEEE Transactions on Nanotechnology*, *410*, 266–274.

Strukov, D. B., Snider, G. S., Stewart, D. R., & Williams, R. S. (2008). The missing memristor found. *Nature*, *453*, 80–83.

Tacha, O., Volos, C. K., Kyprianidis, I. M., Stouboulos, I. N., Vaidyanathan, S., & Pham, V.-T. (2016). Analysis, adaptive control and circuit simulation of a novel nonlinear finance system. *Applied Mathematics and Computation*, *276*, 200–217.

Tong, X., & Cui, M. (2009). Image encryption scheme based on 3d baker with dynamical compound chaotic sequence cipher generator. *Signal Processing*, *89*, 480–491.

Udaltsov, V. S., Goedgebuer, J. P., Larger, L., Cuenot, J. B., Levy, P., & Rhodes, W. T. (2003). Communicating with hyperchaos: the dynamics of a DNLF emitter and recovery of transmitted information. *Optics and Spectroscopy*, *95*, 114–118.

Vaidyanathan, S. (2013). A new six-term 3-D chaotic system with an exponential nonlineariry. *Far East Journal of Mathematical Sciences*, *79*, 135–143.

Vaidyanathan, S., & Azar, A. T. (2015). Analysis and control of a 4-D novel hyperchaotic system. In A. T. Azar & S. Vaidyanathan (Eds.), *Chaos Modeling and Control Systems Design* (Vol. 581, pp. 19–38). Studies in Computational Intelligence Germany: Springer

Vaidyanathan, S., Volos, C., Pham, V. T., Madhavan, K., & Idowo, B. A. (2014). Adaptive backstepping control, synchronization and circuit simualtion of a 3-D novel jerk chaotic system with two hyperbolic sinusoidal nonlinearities. *Archives of Control Sciences*, *33*, 257–285.

Vicente, R., Dauden, J., Colet, P., & Toral, R. (2005). Analysis and characterization of the hyperchaos generated by a semiconductor laser subject to a delayed feedback loop. *IEEE Journal of Quantum Electronics*, *41*, 541–548.

Volos, C. K., Kyprianidis, I. M., & Stouboulos, I. N. (2013). Image encryption process based on chaotic synchronization phenomena. *Signal Processing*, *93*, 1328–1340.

Wang, X., Teng, L., Qin, X., & Novel, A. (2012). Colour image encryption algorithm based on chaos. *Signal Processing*, *92*, 1101–1108.

Yang, J. J., Strukov, D. B., & Stewart, D. R. (2013). Memristive devices for computing. *Nature Nanotechnology*, *8*, 13–24.

Yeung, M. M., & Pankanti, S. (2000). Verification cryptosystems: issues and challenges. *Journal of Electronic Imaging*, *9*, 468–476.

Zhang, L., Liao, X., & Wang, X. (2005). An image encryption approach based on chaotic map. *Chaos, Solitons and Fractals*, *24*, 759–756.